Effects of Fumed Silica on the Crystallization Behavior and Thermal Properties of Poly(hydroxybutyrate-*co*-hydroxyvalerate)

P. M. Ma,[1,2] R. Y. Wang,[1] S. F. Wang,[1] Y. Zhang,[1] Y. X. Zhang,[1] D. Hristova[2]

[1]*State Kay Laboratory of Metal Matrix Composites, School of Chemistry and Chemical Technology, Shanghai Jiao Tong University, Shanghai 200240, China*
[2]*Chemical Engineering and Chemistry Polymer Technology, Eindhoven University of Technology, Eindhoven, The Netherlands*

Received 1 April 2007; accepted 15 October 2007
DOI 10.1002/app.27577
Published online 29 January 2008 in Wiley InterScience (www.interscience.wiley.com).

ABSTRACT: The effects of fumed silica on the crystallization behavior and thermal properties of poly(hydroxybutyrate-*co*-hydroxyvalerate) (PHBV) were investigated. The PHBV/silica composites were prepared by a melt-blending method. The nonisothermal crystallization, melting process, and isothermal crystallization kinetics of PHBV and PHBV/silica composites were characterized with differential scanning calorimetry. The spherulite development and morphology were observed by polarized optical microscopy. In addition, the thermal degradation properties were determined via thermogravimetric analysis. The results indicated that the melting and crystallization kinetics of PHBV were greatly affected by fumed silica, and this was due to the effective nucleation function of silica, which enhanced the crystallization process. The thermal onset degradation temperature of PHBV increased with the addition of fumed silica. © 2008 Wiley Periodicals, Inc. J Appl Polym Sci 108: 1770–1777, 2008

Key words: crystallization; melt; silicas; thermal properties

INTRODUCTION

Bacterially synthesized poly(hydroxybutyrate-*co*-hydroxyvalerate) (PHBV) is a crystalline polymer with complete biodegradability and biocompatibility, and this makes it attractive for applications in biomedical materials and environmentally friendly materials. On the other hand, the application of this material is hindered by some disadvantages such as a high price, narrow processing window, poor thermal stability, and high brittleness. This material is brittle because of the inherent defects in the big spherulites.[1] If the polymers could be crystallized at a higher temperature, a more perfect crystal structure would be obtained. Then, the brittleness of the polymer would be improved, and the physical properties would be enhanced as well.[2,3] As we know, poor thermal stability is a feature of PHBV that makes a long dwell time in the mold to obtain a more perfect crystal structure impractical. PHBV is produced via a bacterial fermentation process with high purity, which results in a low nucleation density. For this reason, a nucleating agent is usually added to increase the temperature and rate of crystallization of PHBV via an enhanced self-seeding mechanism. Withey and Hay[4] studied the effects of nucleating agents such as boron nitride (BN), saccharin, and phthalimide on the crystallization of poly(hydroxybutyrate) (PHB) and PHBV. BN was found to be an effective nucleating agent.

The thermal stability of PHBV is poor, and its thermal degradation can be characterized by thermogravimetric analysis (TGA). It has been reported that clay, carbon nanotubes, and metal oxides, especially MgO, can increase the thermal degradation temperature.[5–7]

Fumed silica is a kind of inorganic nanofiller with many reactive groups on its surface. It has been widely used in controlling rheology and thixotropy properties and as an effective reinforcement agent for rubber materials. On the other hand, fumed silica can also be used as a nucleating agent in crystalline polymers.

In this study, biodegradable PHBV/silica nanocomposites were fabricated and characterized with differential scanning calorimetry (DSC), polarized optical microscopy (POM), and TGA. The effect of fumed silica on the crystallization, melting, and thermal degradation properties were studied.

EXPERIMENTAL

Materials and sample preparation

A biodegradable PHBV copolymer in the form of a white powder was provided by Tianan Biologic Material Co., Ltd. (Ningbo, China). The content of β-

Correspondence to: Y. Zhang (yong_zhang@sjtu.edu.cn).

hydroxyvalerate in the copolymer was 1.13 mol %, as measured by nuclear magnetic resonance (NMR) (Mercury Plus 400, Varian, Inc., Palo Alto, CA). The viscosity-average molecular weight of the copolymer was 130,000, as measured at 30°C with chloroform as a solvent in an Ubbelohde viscometer via the following function: $[\eta] = KM^{\alpha}$.

Where η, is intrinsic viscosity, M is viscosity-average molecular weight, and K and α are constant parameters.

Fumed silica (A200) was supplied by Evonik Degussa GmbH (Shanghai, China) with a specific surface area of 200 m^2/g. The diameters of the silica particles were between 10 and 25 nm.

Both PHBV and fumed silica were treated in a vacuum oven (0.021 MPa) for 24 h at 80°C, and then the samples were prepared in a Rheocord 90 Haake rheometer (Mess-Technic GmbH, Offenburg, Germany) under the conditions of 165°C, 40 rpm, and 10 min. After that, the samples were sealed and stored for use at room temperature.

Field emission scanning electron microscopy (FESEM)

The PHBV/silica composite specimen (the silica content was 2%) was fractured at a very low temperature in liquid nitrogen. The dispersion of silica in the PHBV matrix was investigated from the fracture surface with FESEM (JSM-7401F, JEOL, Ltd., Tokyo, Japan). A very thin layer of gold was sputter-coated onto the fracture surface to make it electrically conductive.

POM

The spherulitic morphology and growth rate were monitored with a Leica DM LP polarized optical microscope (Leica Microsystems GmbH, Mannheim, Germany). The sample was first heated from room temperature to 200°C at a heating rate of 50°C/min, held for 3 min at 200°C, and then quickly cooled to the desired crystallization temperature (T_c) of 104°C at a cooling rate of 60°C/min, where spherulitic growth was monitored. Micrographs were taken at intervals for measuring the spherulite radii at various times. The growth rate (R) was calculated by the change in the spherulitic radius (r) with time: $R = dr/dt$.

DSC

Crystallization and melting behaviors of PHBV and PHBV/silica composites were investigated with DSC (Pyris 1, PerkinElmer, Inc., Waltham, MA). The samples were first heated from room temperature to 200°C at a rate of 20°C/min under a nitrogen atmosphere and held for 3 min at 200°C to erase the thermal history. Then, the samples were cooled to −20°C at a rate of 10°C/min and heated to 200°C again at a rate of 10°C/min. The second and third DSC run curves were marked to estimate the nonisothermal crystallization and melting behaviors. To study the two-peak behavior, different heating rates (5, 10, 20, and 40°C/min) were used.

New samples were first heated from room temperature to 200°C at a rate of 20°C/min under a nitrogen atmosphere and held in the melt state for 3 min to destroy any residual nuclei. Then, the samples were cooled to various desired T_c values (i.e., 96, 98, 100, 102, 104, and 106°C) at a cooling rate of 100°C/min. The isothermal crystallization exotherms of these samples were analyzed to estimate the isothermal crystallization kinetics.

TGA

TGA of samples was carried out with a TGA 7 analyzer (PerkinElmer, Waltham, MA). The mass of each specimen was about 3 mg, and the atmosphere was nitrogen (40 mL/min). The rate of temperature increase was 20°C/min. TGA curves were recorded in the course of heating from room temperature to 600°C.

RESULTS AND DISCUSSION

Morphology of the PHBV/silica composites

The dispersion of fumed silica particles in the PHBV matrix was studied with field emission scanning electron microcopy (JSM-7401F, JEOL). The morphology of the neat silica particles is shown in Figure 1(c), and the morphology of the PHBV/silica composite (silica, 2 wt %) is shown in Figure 1(a,b). The silica particle size was mainly between 10 and 25 nm, as shown in Figure 1(c). The fumed silica dispersed uniformly in the copolymer matrix, and there was no obvious aggregation of fumed silica in the samples, although the surface was not treated. Figure 1(b) shows clearly that the fumed silica particles were partly embedded in the copolymer matrix and that the silica particle size in the PHBV matrix was no more than 50 nm.

Nonisothermal crystallization and melt behavior

Figures 2 and 3 show the cooling and melting DSC curves of PHBV composites with different silica contents. All parameters were derived from the thermal analysis curves; the melting temperature (T_m), T_c, normalized melting enthalpy (ΔH_m), crystallization enthalpy (ΔH_c), and crystallinity (C_r) values of PHBV and PHBV/silica composites are summarized in Table I. The C_r values of PHBV and PHBV/silica composites can be calculated via eq. (1):

$$C_r = (\Delta H/\Delta H_0) \times 100\% \quad (1)$$

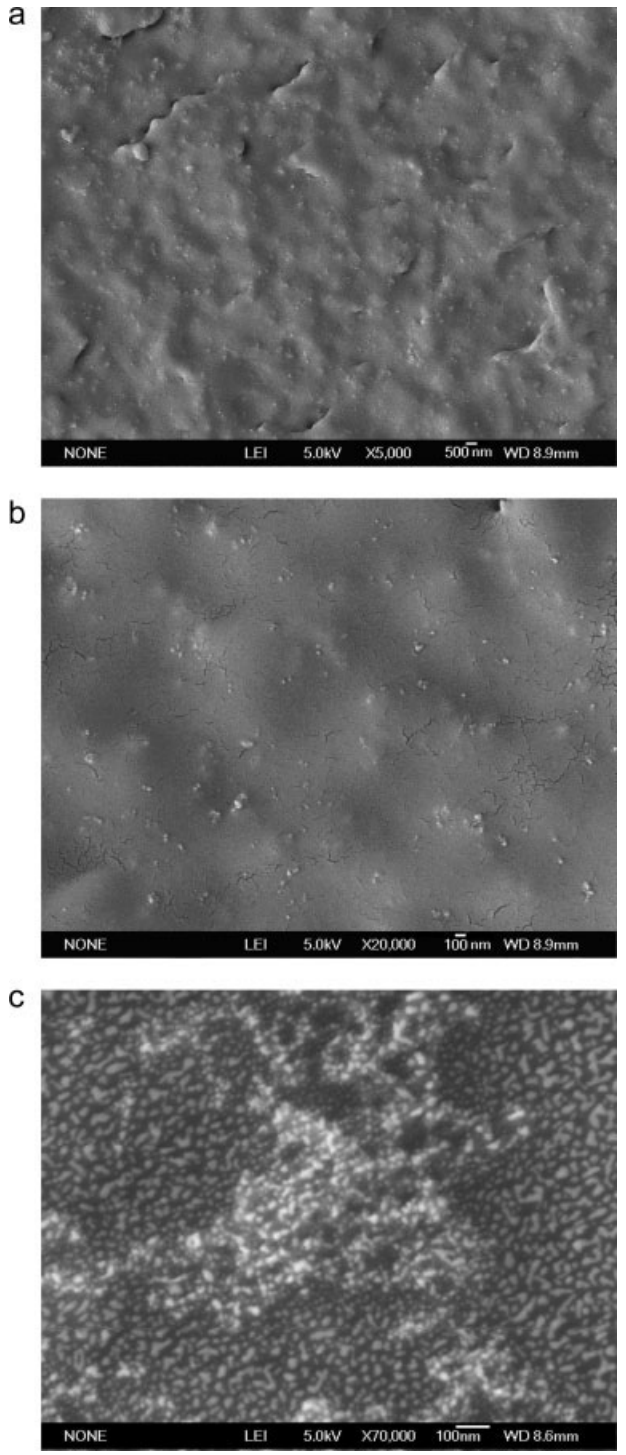

Figure 1 FESEM images of silica and a PHBV/silica composite (2 wt % silica): (a) composite with an original magnification of 5000×, (b) composite with an original magnification of 20,000×, and (c) neat silica with an original magnification of 70,000×.

where ΔH_0 is the thermodynamic enthalpy of fusion per gram of PHB (146.6 J/g)[8] and ΔH is the apparent enthalpy of crystallization (ΔH_c) or fusion (ΔH_m) per gram of PHBV with different silica contents.

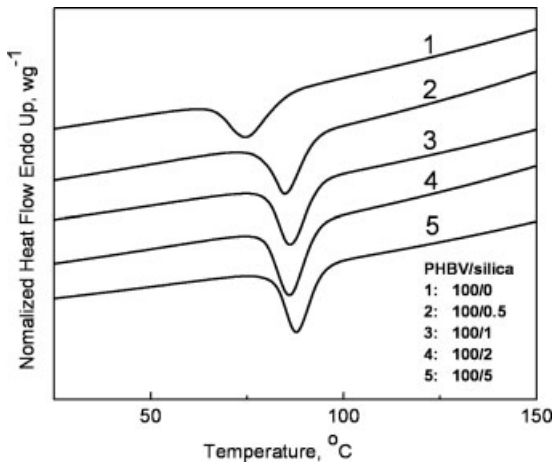

Figure 2 Nonisothermal crystallization DSC curves of PHBV and PHBV/silica composites at a cooling rate of 10°C/min.

The T_c values of all the PHBV/silica composites were more than 10°C higher than that of the neat PHBV, which was 74.8°C. With increasing silica content, T_c increased slightly. The data for T_c and crystallinity of PHBV calculated via ΔH_c (C_{rc}) in Table I indicate that C_{rc} of PHBV could be increased remarkably by the addition of even a very small amount of silica. It also shows that silica could enhance the overall crystallization rate because of the heterogeneous nucleation function. In the crystallization process, silica acted as a nucleating agent, increasing the nucleation density and changing the crystallization dynamics of PHBV and PHBV/silica composites. When the content of silica in the PHBV/silica composites was too high, C_{rc} decreased, possibly because superfluous silica acted as an impurity, blocking or destroying the crystallization.

All the samples showed two peaks during melting (Fig. 3). When the two-peak behavior is interpreted, it is important to distinguish multiple peaks caused

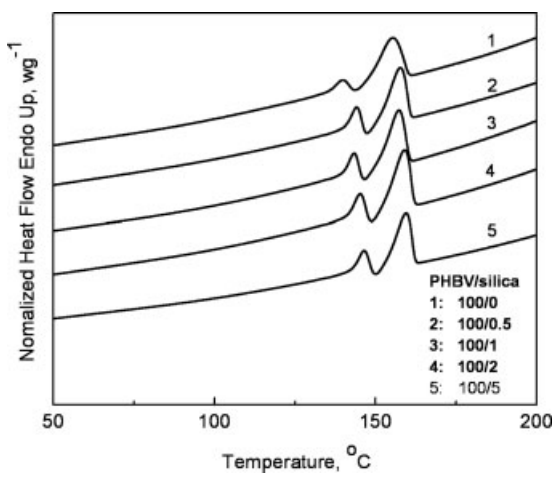

Figure 3 Second-run melting DSC curves of PHBV and PHBV/silica composites at a heating rate of 10°C/min.

TABLE I
Thermal Analysis Parameters of PHBV and PHBV/Silica Composites

	Nonisothermal cooling[a]			Melting[b]		
PHBV/silica (wt/wt)	T_c (°C)	ΔH_c (J/g)	C_{rc} (%)	T_m (°C)	ΔH_m (J/g)	C_{rm} (%)
100/0	74.8	54.2	37.0	155.2	79.1	54.0
100/0.5	85.0	60.3	41.1	157.5	88.0	60.1
100/1	86.2	65.5	44.7	157.2	88.3	60.2
100/2	86.0	76.0	51.8	158.8	95.4	65.1
100/5	87.8	63.5	43.3	159.5	79.1	54.0

[a] Obtained from the nonisothermal cooling process at a given cooling rate of 10°C/min.
[b] Obtained from the second heating process at a given heating rate of 10°C/min.

either by phase-separated structures or by a result of a melt/recrystallization process. Two endothermic peaks are often observed on the melting curve of semicrystalline polymers and polymer blends. The lower of the two endothermic peaks is usually regarded as unstable and not perfect crystal, whereas the higher is regarded as a stable and perfect one.[6,9] This result can be easily proved by DSC heating scans at different heating rates. It is apparent that the relative area of the lower temperature peak increased with increasing heating rate; meanwhile, the ratio of the two peaks (the lower temperature peak area to the higher temperature peak area) also increased obviously, as shown in Figure 4 and Table II. This phenomenon resulted from a melt/recrystallization process. At a slow heating rate, the less perfect crystals had enough time to melt and reorganize into crystals with higher structural perfection and then remelt at a higher temperature. Two melt peaks were also observed in the heating of poly(lactic acid) (PLA). Jiang et al.[10] pointed out that the structure of the lower peak was the same form as the high-temperature one but with a lower lamellar thickness.

In addition, both the crystallization and melting peaks of the PHBV/silica composites were narrower than those of PHBV, indicating a narrower crystal size distribution in the composites than in PHBV.

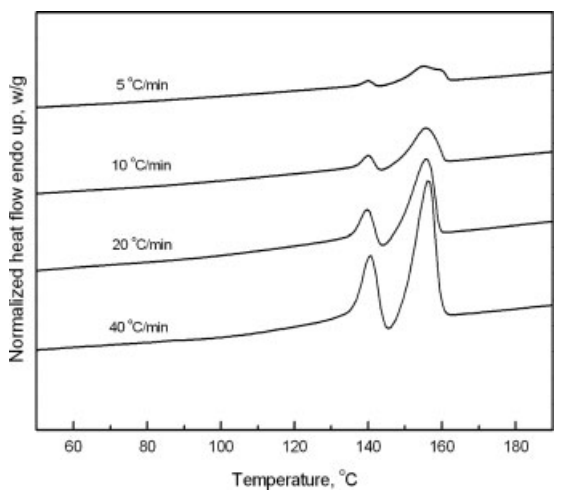

Figure 4 Second heating curves of PHBV and PHBV/silica composites with different heating rates.

Isothermal crystallization kinetics

Figure 5(a,b) shows the temporal development of the relative degree of crystallinity (X_t) of PHBV and PHBV/silica composites in the isothermal crystallization process at various values of T_c. X_t is obtained from the exotherm via the following function:

$$X_t = \frac{\int_0^t (\frac{dH}{dt})dt}{\int_0^\infty (\frac{dH}{dt})dt} \quad (2)$$

where the numerator represents the exotherm area at time t and the denominator is the total exotherm area.

The half-time of crystallization ($t_{0.5}$), defined as the time required to attain half of the final crystallinity, was evaluated from the X_t curves. The overall crystallization rate (G) can be represented by $G = 1/t_{0.5}$. The variation of the overall crystallization rates of PHBV and PHBV/silica composites with T_c is displayed in Figure 6. It is well known that the crystallization window of a crystalline polymer must lie between the glass-transition temperature (T_g) and T_m. When the desired T_c value is located toward T_g, the crystallization kinetics will be controlled by the chain mobility, so that the crystallization rate increases with increasing T_c. In contrast, if the

TABLE II
Thermal Parameters of Two Melting Peaks of PHBV During the Second Heating Scan

Heating rate (°C/min)	Area 1 (J/g)	Area 2 (J/g)	Area 1/Area 2 (%)
5	7.71	64.4	12.0
10	8.35	60.2	13.9
20	13.5	58.3	23.2
40	22.3	49.9	44.7

Area 1 represents the area of the lower temperature peak; area 2 represents the area of the higher temperature peak.

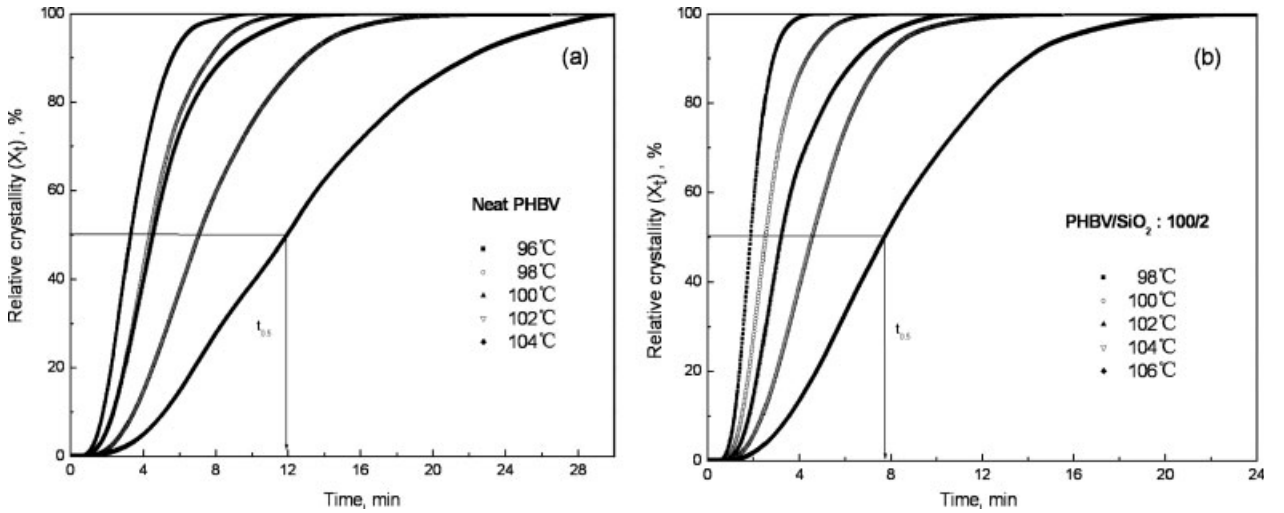

Figure 5 Isothermal crystallization curves of PHBV and PHBV/silica composites at different values of T_c: (a) neat PHBV and (b) PHBV/silica composites.

desired T_c value is located toward T_m, the crystallization rate will be governed by the thermodynamic driving force of crystallization. There is a maximum in the crystallization rate at a certain temperature (T_c^{max}) between T_g and T_m due to the interplay between the two factors. For PHB or PHB blends, T_c^{max} was reported to be in the neighborhood of 90°C.[11,12] In this work, all the T_c values were higher than 90°C, so the overall crystallization rates were controlled by a nucleation mechanism. In the figure, it can be seen that the overall crystallization rate dramatically decreased with increasing T_c for a given sample composition, and the overall crystallization rate of the PHBV/silica composite was markedly higher than that of neat PHBV. It also suggests that silica had an effective heterogeneous nucleation function, which promoted the crystallization.

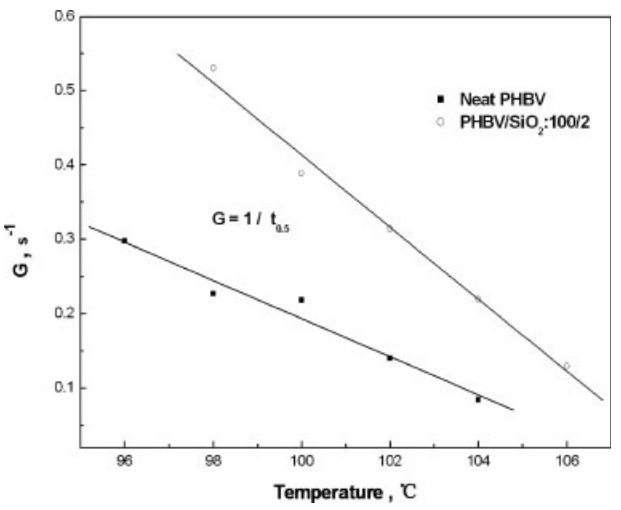

Figure 6 Variation of G with T_c for PHBV and PHBV/silica composites.

The overall crystallization rate and crystallization kinetics can be further described by the Avrami equation:[13–15]

$$\ln[-\ln(1 - X_t)] = \ln k + n \ln t \tag{3}$$

where k is the overall crystallization rate constant, containing contributions from both nucleation and growth rates; n is the Avrami exponent, which depends on the nucleation and growth mechanism; and X_t is the relative crystallinity at a certain time t, as mentioned previously. The plot of $\ln[-\ln(1 - X_t)]$ versus $\ln t$ fits a linear line, with the intercept and slope given by $\ln k$ and n, respectively. It can be seen that the experimental data roughly agree with the Avrami equation.

All parameters derivable from the isothermal crystallization curves of the neat PHBV and PHBV/silica composite at a given value of T_c are summarized in Table III.

The n values were about 2.5 and almost independent of the given value of T_c. The values of n obtained in this experiment were all less than 3, and this may have been caused by the occurrence of second crystallization[16] and spherulites not always growing absolutely spherically and symmetrically, as observed with POM. A similar result for PHB blends was also reported by Withey and Hay.[4] It may roughly confirm three-dimensional spherulitic growth initiated by heterogeneous nucleation, although all the values of n were less than 3, which is consistent with the spherulitic morphology and crystallization process observed by POM.

The dependence of the crystallization rate on T_c and the influence of silica on the crystallization can be described by the k–T_c curves too. The results shown in Figure 7 provide further evidence for the

TABLE III
Isothermal Crystallization Analysis Parameters of PHBV and PHBV/Silica Composites

Temperature (°C)	Neat PHBV				PHBV/silica (100/2)			
	n	$K \times 10^3$ ($\min^{-n}$)	t_{max} (min)	X_{tmax} (%)	n	$K \times 10^3$ ($\min^{-n}$)	t_{max} (min)	X_{tmax} (%)
96	2.58 ± 0.02	23.6	2.65	30.6	—	—	—	—
98	2.67 ± 0.01	9.70	3.77	36.8	2.76 ± 0.02	101	1.70	38.9
100	2.28 ± 0.01	15.5	3.68	34.1	2.55 ± 0.02	46.7	2.30	39.1
102	2.54 ± 0.01	3.50	5.38	29.6	2.30 ± 0.02	30.4	2.65	33.7
104	2.38 ± 0.01	1.80	6.95	21.3	2.54 ± 0.01	10.8	3.83	36.2
106	—	—	—	—	2.43 ± 0.01	4.00	6.08	33.9

crystallization process being controlled by the heterogeneous nucleation course, as well as the silica acting as an evident nucleation agent.

The maximum crystallization time (t_{max}), defined as the time needed from the beginning of crystallization to the maximum crystallization rate, is usually used to describe the overall crystallization rate in the study of isothermal crystallization kinetics. As we know, the larger t_{max} is, the smaller the crystallization rates are at a certain T_c. The values of t_{max} at different T_c values can be calculated via the following equation:

$$t_{max} = \left[\frac{n-1}{nk}\right]^{1/n} \quad (4)$$

where n and k are obtained from eq. (3). The relationship between t_{max} and T_c is shown in Figure 8, which also proves the results of Figures 5 and 6.

Spherulitic morphology and growth rate

The development of crystallization within the neat PHBV and PHBV/silica composite was followed with a polarized optical microscope. The spherulitic morphologies of the neat PHBV and PHBV/silica composite at a certain time in the isothermal crystallization process are shown in Figure 9. Only large spherulites were observed in the PHBV/silica composite on crystallization, similar in morphology to those observed in neat PHBV. The diameters of both kinds of spherulites were more than 3 mm finally under the testing condition. Bond spacing was observed in both of the spherulites, but they were thinner and smoother in the PHBV/silica composite. It has also been reported that the band spacing is connected to the blending composition and T_c.[8,17]

The PHBV spherulitic radii in the initial process were measured at a constant temperature of 104°C in the presence and absence of 2 wt % silica. Figure 10 displays the variation of the spherulitic radii with the crystallization time and shows that the radii of the spherulites grew linearly with time in both cases. The rate of spherulite growth can be represented by the slopes of the linear lines. As shown in Figure 10, the rate of spherulite growth in PHBV was very similar to that in the PHBV/silica composite. In addition, the overall crystallization rate of the PHBV/silica composite was obviously higher than that of neat PHBV, whereas the spherulitic radial growth

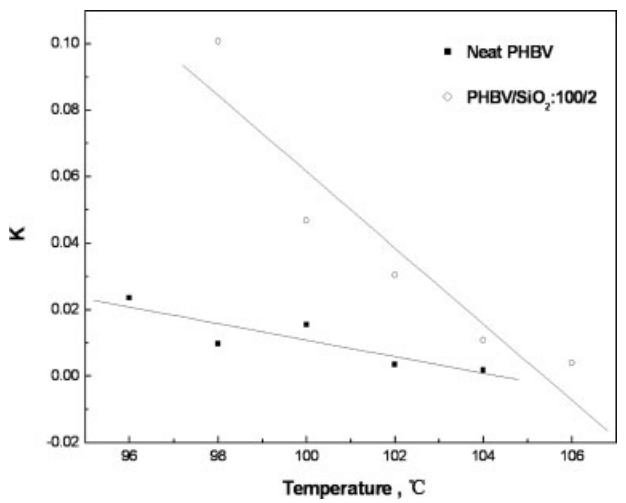

Figure 7 Variation of K with T_c for PHBV and PHBV/silica composites.

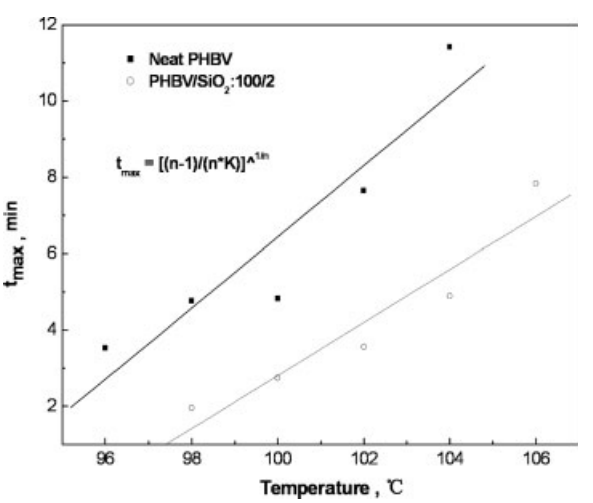

Figure 8 Variation of t_{max} with T_c for PHBV and PHBV/silica composites.

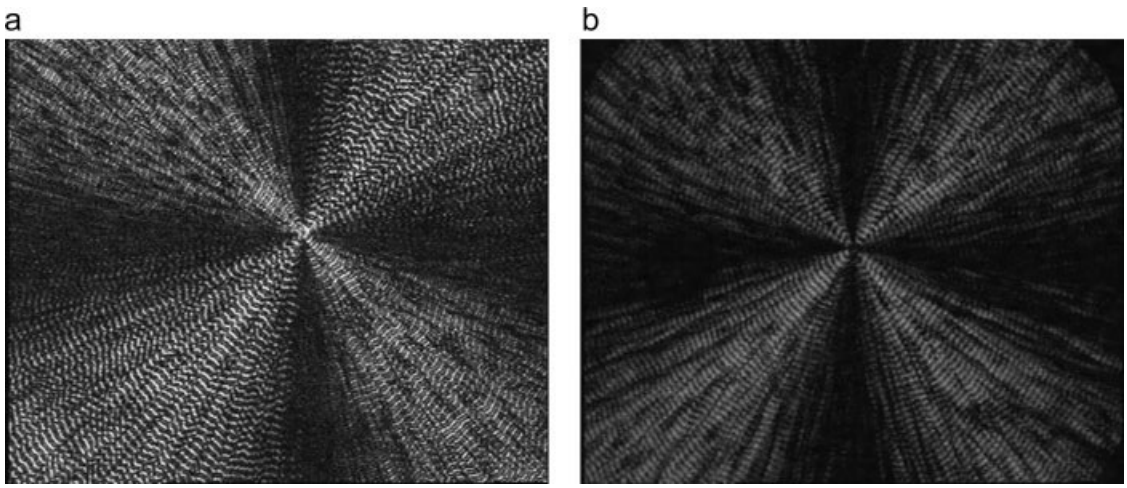

Figure 9 Spherulitic morphology of PHBV and PHBV/silica composites by POM crystallized at 104°C: (a) spherulitic morphology of neat PHBV and (b) spherulitic morphology of PHBV/silica composites.

rates of the two materials were similar; this means that the overall crystallization kinetics are mainly controlled by a nucleation mechanism and that the overall crystallization rate is mainly governed by the nucleation rate and nucleation density at the experiment temperature.

Thermal analysis

The thermal degradation properties of the PHBV and PHBV/silica composite were assessed with thermogravimetry at a heating rate of 20°C/min under a nitrogen flow, and the results are shown in Figure 11.

There was only one stage of weight loss in TGA of the PHBV/silica composites, and the thermal degradation window was narrow. The thermal degradation temperature was higher with an increase in fumed silica. The thermal onset degradation temperatures were determined to be 279.53°C for PHBV and 288.92°C for the PHBV/silica composite (5 wt % silica), which was nearly 10°C higher than that of PHBV. Choi et al.[5] studied PHBV/nanoclay systems and reported an improvement in the thermal stability observed for nanocomposites related to the nanodispersion and layered structure of the clay in the PHBV matrix, which was thought to be an effective barrier to the permeation of oxygen and combustion gas. The thermal stability of PHB/inorganic oxide systems[7] also increased especially for PHB/MgO composites and led to the significant formation of a considerably more stable product based on the interactions of MgO with PHB end groups. Fumed silica is a nanosize inorganic filler with plenty of hydroxyls on its surface. On the basis of the previous

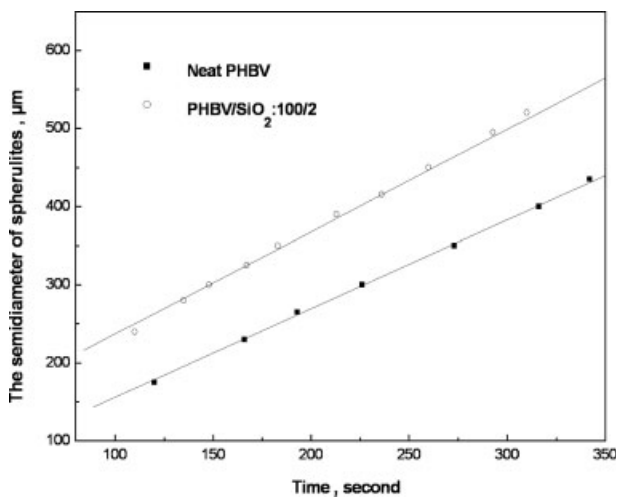

Figure 10 Variation of the semidiameter with the crystallization time for PHBV and PHBV/silica composites.

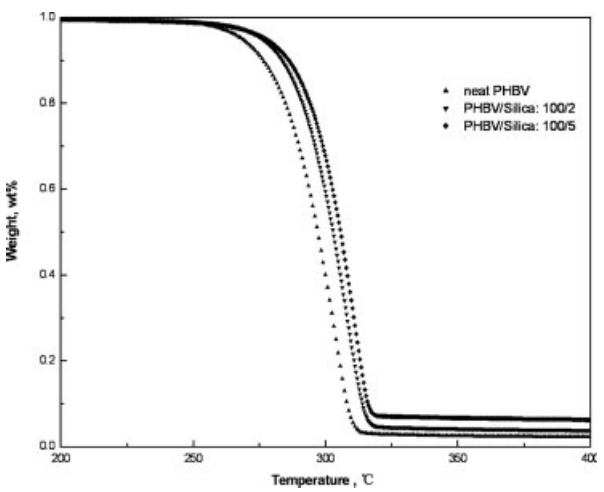

Figure 11 TGA curves of PHBV and PHBV/silica composites with various silica contents.

investigation,[5,7] the increase in the thermal degradation temperature of PHBV after the addition of silica observed in this work could be due to the similar reasons mentioned previously.

CONCLUSIONS

Uniformly dispersed PHBV/silica composites were obtained through a melt-blending method in a Haake rheometer. Fumed silica could increase T_c (ca. 13°C) and crystallinities of PHBV. Both the neat PHBV and PHBV/silica composites showed that perfect and not perfect crystals existed at the same time. In the melting process, T_m increased even at low silica contents. A three-dimensional spherulitic growth was roughly confirmed through studying the isothermal crystallization kinetics and observing the crystallization process by POM. The crystallization kinetics were controlled by a nucleation mechanism, and silica had an effective heterogeneous nucleation effect that markedly promoted the crystallization process and increased the crystallization rate according to a comparison of $t_{0.5}$, t_{max}, and K values at different T_c values and the spherulitic growth rates at 104°C for the pure PHBV and PHBV/silica composite. The thermal onset degradation temperature of the PHBV/silica composite was about 10°C higher than that of pure PHBV on the basis of TGA, indicating that the thermal stability of PHBV could be improved by the addition of the fumed silica.

References

1. Hobbs, J. K.; Mcmaster, T. J.; Miles, M. J.; Barham, P. J. Polymer 1996, 37, 3241.
2. Biddlestone, F.; Harris, A.; Hay, J. N.; Hammond, T. Polym Int 1996, 39, 221.
3. de Koning, G. J. M.; Lemstra, P. J. Polymer 1993, 34, 4089.
4. Withey, R. E.; Hay, J. N. Polymer 1999, 40, 5147.
5. Choi, W. M.; Kim, T. W.; Park, O. O.; Chang, Y. K.; Lee, J. W. J Appl Polym Sci 2003, 90, 5259.
6. Lai, M.; Li, J.; Yang, J.; Liu, J.; Tong, X.; Cheng, H. Polym Int 2004, 53, 1479.
7. Csomorová, K.; Rychlý, J.; Bakoš, D.; Janigová, I. Polym Degrad Stab 1994, 43, 441.
8. Barham, P. J.; Feller, A.; Otun, E. L.; Holmes, P. A. J Appl Polym Sci 1984, 19, 2781.
9. Yoshie, N.; Fujiwara, M.; Ohmori, M.; Inoue, Y. Polymer 2001, 42, 8557
10. Jiang, L.; Wolcott, M. P.; Zhang, J. Biomacromolecules 2006, 7, 199.
11. Abe, H.; Matsubara, I.; Doi, Y. Macromolecules 1995, 28, 844.
12. Lotti, N.; Pizzoli, M.; Ceccorulli, G. Polymer 1993, 349, 4935.
13. Avrami, M. J. J Chem Phys 1939, 7, 1103.
14. Avrami, M. J. J Chem Phys 1940, 8, 212.
15. Avrami, M. J. J Chem Phys 1941, 9, 177.
16. Grenier, D.; Leborgne, A.; Spassky, N.; Prud'homme, R. E. J Polym Sci 1981, 19, 33.
17. Penning, J. P.; St. John Manley, R. Macromolecules 1996, 29, 84.